PERFORMANCE TESTS OF BRAGG CURVE SPECTROSCOPY (BCS) DETECTOR USING $^{4}He + ^{27}Al$ REACTION AT 104 MeV ENERGY

A. A. Naqvi* and A. H. Al-Ramadhan

Department of Physics
King Fahd University of Petroleum & Minerals
Dhahran, Saudi Arabia

الخلاصـــة :

تُمَّ قياس قدرة تحديد الشحنة والطاقة لكاشف طيف منحنى براق للأيونات الخفيفة الناتجة عن تفاعل $^{4}He + ^{27}Al$ عند طاقة (١٠٤) مليون اليكترون ڤولت. وقد لوحظ أن مسار الجسيمات المائل يؤثر في أداء الكاشف بدرجة كبيرة. وقد جرى قياس قدرة تحديد الشحنة لهذا الكاشف لأيونات كل من ^{4}He, ^{7}Li, ^{9}Be, ^{11}B, ^{12}C, ^{14}N, ^{16}O وكان أفضل قياس يساوي (٢,٧ + ٠,٥) ٪ لأيونات ^{7}Li, ^{9}Be وفي المقابل كانت قدرة تحديد الشحنه ^{16}O تساوي (٤,١ + ٠,٤) ٪.

أما بالنسبة لقدرة تحديد الطاقة لهذا الكاشف فقد تم قياسها لجسيمات (ألفا) ذات طاقة (٥,٢) الى (٥,٨) مليون اليكترون ڤولت ووجدت بأنها تساوي (١,٥) ٪.

وأخيرا فان جميع النتائج المتوصل اليها في هذه التجربة متوافقة مع ما نشر في هذا المجال.

ABSTRACT

The charge and energy resolution of a BCS detector was measured for light ions produced in $^{4}He + ^{27}Al$ reaction at 104 MeV energy. It was found that oblique tracks influence the detector performance significantly. The charge resolution of BCS detector has been measured for ^{4}He, ^{7}Li, ^{9}Be, ^{11}B, ^{12}C, ^{14}Na, and ^{16}O ions. The best charge resolution measured for the above mentioned ions was 2.7 + 0.5% and was for ^{7}Li and ^{9}Be ions. On the other hand, charge resolution measured for ^{16}O was 4.1 + 0.4%. The energy resolution of the BCS detector measured for 5.2–5.8 MeV alpha particles was 1.5%. The data obtained in this experiment are found to be consistent with the published results.

* Address for Correspondence:
KFUPM Box No. 1815
King Fahd University of Petroleum & Minerals
Dhahran 31261, Saudi Arabia

PERFORMANCE TESTS OF BRAGG CURVE SPECTROSCOPY (BCS) DETECTOR USING $^{4}He + ^{27}Al$ REACTION AT 104 MeV ENERGY

1. INTRODUCTION

In nuclear reactions induced by heavy ions, the mass, kinetic energy, charge, and angular distribution of the reaction products provide valuable information about the reaction mechanism. The growing interest in heavy ion physics over recent years has led to considerable advances in detection and identification of heavy ions. Ion identification has been achieved in different experiments [1–3] using $E - \Delta E$ telescopes, where the E and ΔE detectors are usually semiconductor detectors. Due to their limited size and sensitivity to radiation damage, semiconductor detectors have their own limitations.

In recent years, gas-filled ionization chambers have acquired increasing importance for charge identification in heavy ion spectroscopy. An ionization chamber has several advantages over its counterpart $E - \Delta E$ telescope, namely, insensitivity to radiation damage, availability in large and small sizes, stability of operation, and low cost of operation and maintenance. An excellent review on ionization chambers has been made by Fulbright [4].

An ionization chamber, called a Bragg Curve Spectroscopy (BCS) detector, has been developed for particle identification [5–7]. The BCS detector provides simultaneous informations about energy and charge of the interacting particle. The BCS detector has been tested so far in various experiments [5–7]. The summary of the results of these experiments is shown in Table 1. As is obvious from Table 1, data are available on the detector response for heavy ions with atomic number Z greater than 9. No data are available on BCS detector response for heavy ions with Z less than 10. In order to cover this Z range we have carried out BCS detector performance tests using heavy ions with Z less than 10, produced in the $^{4}He + ^{27}Al$ reaction at 104 MeV of projectile energy. In this paper we report on the experiment. First we discuss the theory of the BCS detector, this is followed by experimental details and finally we discuss the results of our tests.

2. THEORY OF BCS DETECTOR

2.1 Bragg Curve Spectroscopy

The theory of the BCS detector is described in detail in reference [9] but for the sake of continuity, the principle of the BCS detector will be discussed briefly here. A plot of the specific energy loss along the length of the track of a charged particle is known as a Bragg curve. As the heavy ion enters the medium, its velocity is very high and it loses almost a constant amount of energy in the beginning of its track. After slowing down, the amount of energy loss keeps increasing until it reaches a maximum where it drops sharply. The drop is due to electron pickup by the heavy ion, which reduces its instant charge. The maxima in the specific energy loss curve near the end of particle range is called a "Bragg Peak". Figure 1

Table 1. Summary of Results of Tests of BCS Detectors.

Ref.	Ions	Ion Energy (MeV)	Resolutions (%)		Det. Gas	Gas pressure (torr)
			E	Z		
Gruhn et al. [5]	^{20}Ne	100	1.2	1.6 at $Z = 10$	$Ar + CH_4$ 93:7 ratio	300
				1.4 at $Z = 26$	$Ar + CH_4$	270
Schiessel et al. [6]	^{32}S	130	0.4	1.2 at $Z = 16$	$Ar + CH_4$ 90:10 ratio	456
Asselineau et al. [7]	^{40}Ar	300	0.8	2.7 at $Z = 18$	Isobutane	170

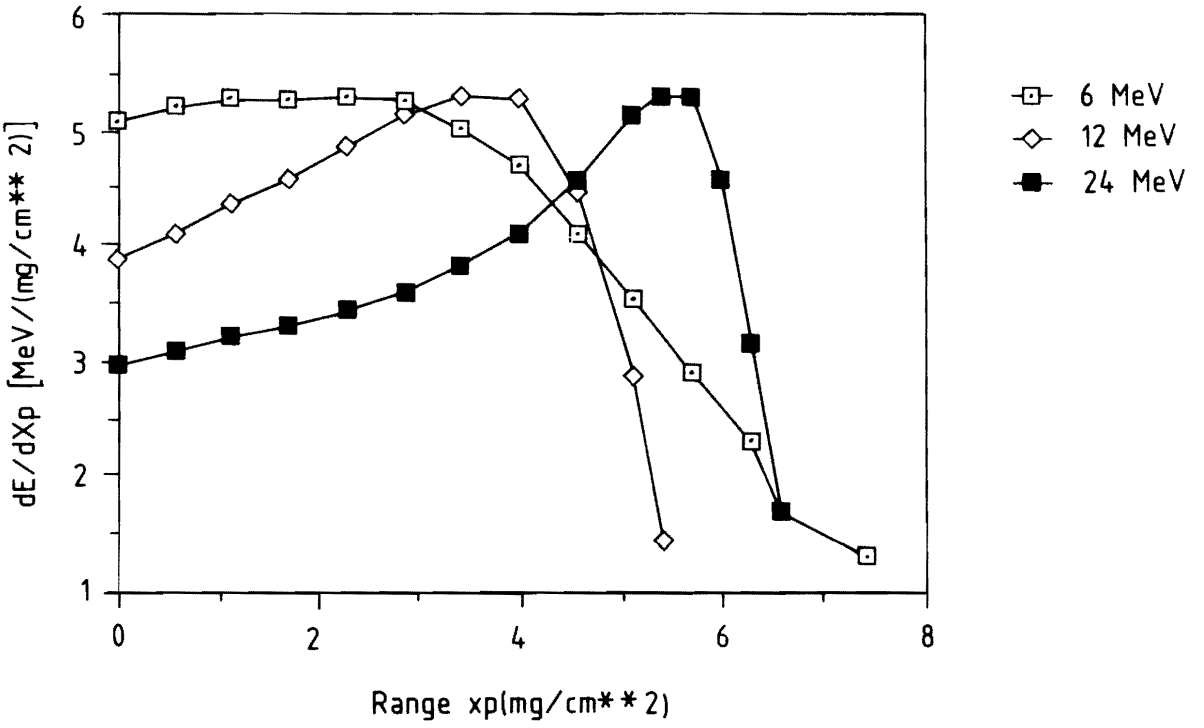

Figure 1. The Bragg Curve for Carbon Ions in Argon gas.

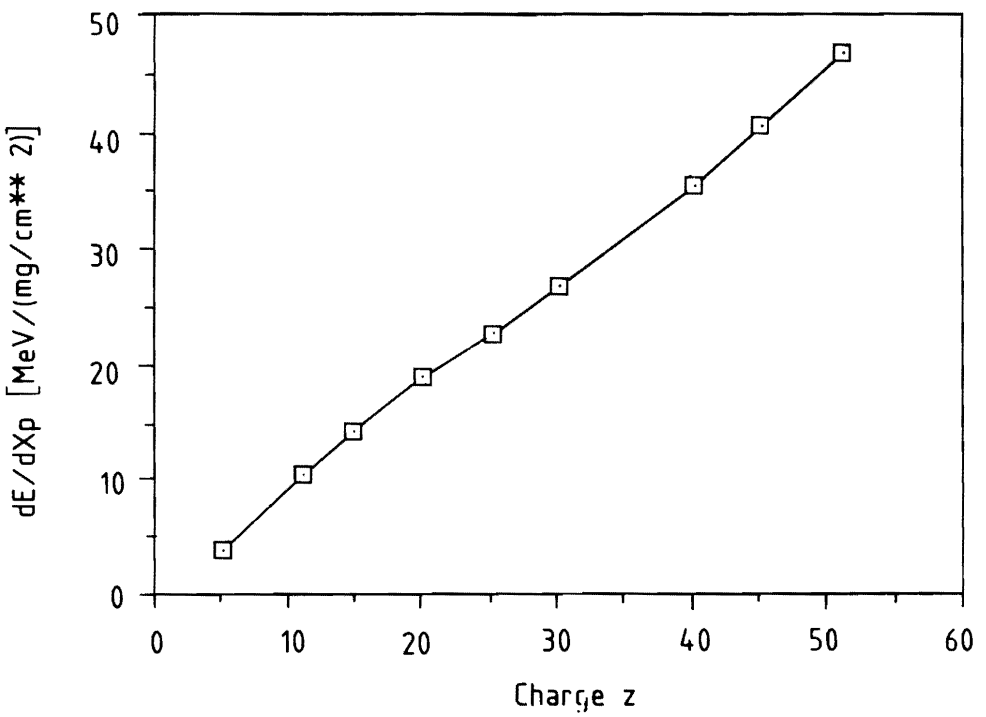

Figure 2. Relationship between the maximum energy loss (Bragg peak maxima) and heavy ion charge Z.

shows the specific energy loss ($dE/dx\varrho$) of carbon ions as function of their range ($x\varrho$) in argon gas at 6, 12, and 24 MeV energies of the carbon ions. It is obvious from Figure 1 that the Bragg peak does not develop if an ion has energy less than 1 MeV/amu. The height of the Bragg peak in a given medium is directly proportional to Z for the heavy ion and is independent of its energy. This characteristic of the Bragg peak is shown in Figure 2 where the height of the Bragg peaks for various ions in argon is plotted as a function of Z for the heavy ion. Data for Figures 1 and 2 were taken from reference [8].

From the shape of the Bragg curve for heavy ions, as shown in Figure 3, one can derive much valuable information about the range, charge, and kinetic energy of the heavy ion. The length of the curve determines the range R of ions while the height of the Bragg peak give the charge of the heavy ion. The area under the Bragg curve gives the total kinetic energy of the heavy ion. One analyzes the Bragg curve signal in terms of its length, height, and area under the curve, using electronics. This is the fundamental principle of Bragg Curve Spectroscopy.

2.2 Principle of Operation of BCS Detector

The BCS detector is basically a Frisch grid ionization chamber and is described in detail in reference [4]. In an ionization chamber, the electric field lines

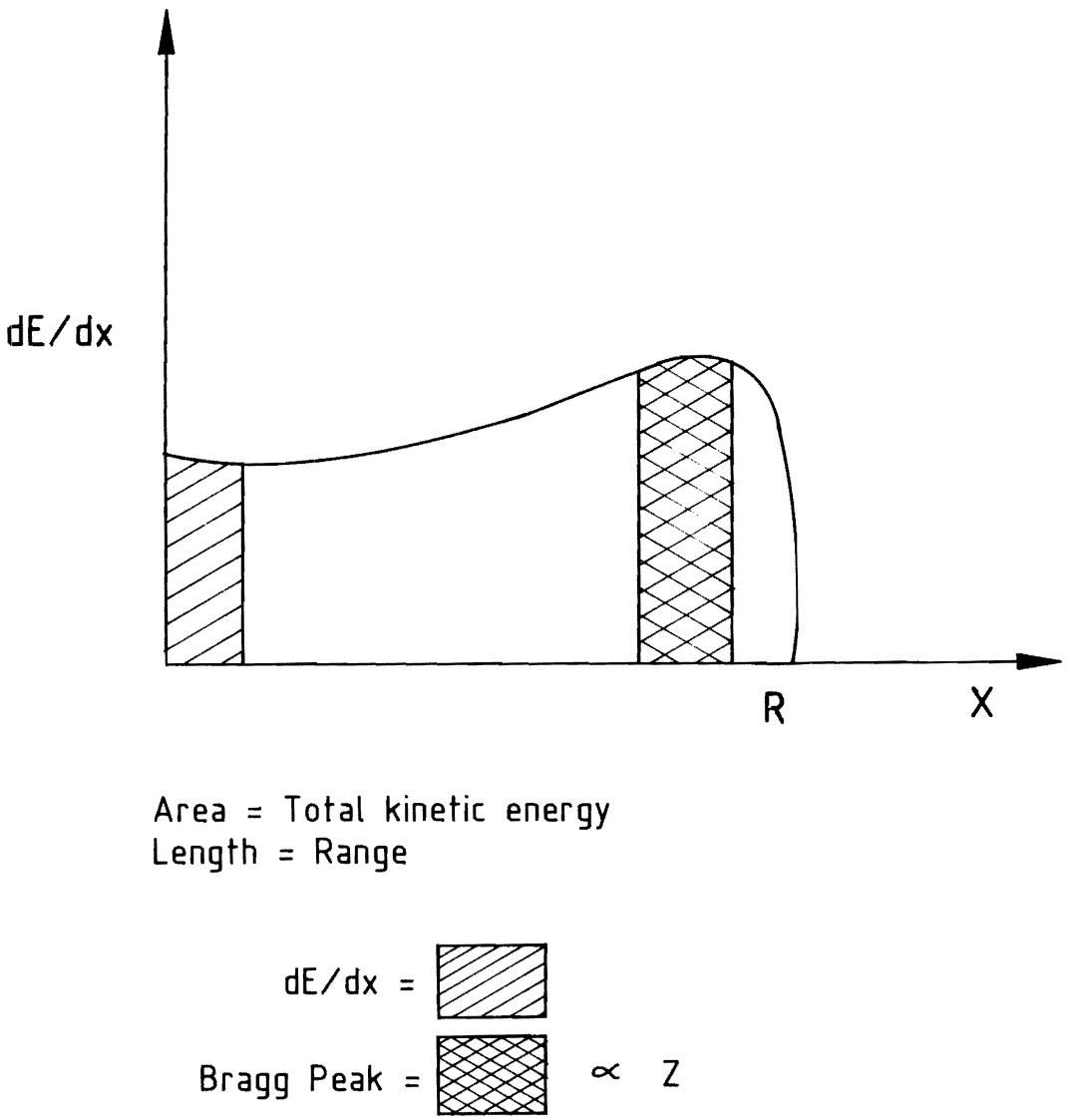

Figure 3. The shape of the Bragg curve for heavy ion below which are the various information one can get from the curve i.e. the length of the curve represents the range of the heavy ion. The height of the bragg peak is proportional to the charge and the integral of the curve is proportional to the energy.

are arranged parallel to the particle trajectory. The ions enter the chamber through a thin window in the cathode and produces ionization track in the active volume of the detector. Due to the homogenous electric field existing between cathode and anode of the detector, the charges produced in the ionization process drift with a constant speed towards the corresponding electrodes. The position dependence of pulse height signal faced in a conventional ionization chamber is overcome by placing a grid (called Frisch grid) in front of the anode. In a Frisch grid chamber, the anode sees the electron coming from the grid only. The signal will depend only on the number of electrons collected by the anode. The electrons produced near the end of the ionization track will arrive at the anode earlier than those electrons which were produced at the beginning of the ionization track. Therefore the signal shape at the grid-screened anode is expected to be an exact mirror image of the Bragg peak of the heavy ions. Strictly speaking, this is only true if the distance between the Frisch grid and the anode is small compared to the range of the ion. The anode signal is processed by electronics with suitable shaping time.

2.3. Limitations of the BCS Detector

The BCS detector can measure the true energy and charge of an incident particle if it satisfies the following conditions:

The particle should enter the active volume of the detector in a direction parallel to the electric field. If the incidence angle of a particle with respect to the electric field direction is large, it may not be stopped fully in the detector and the detector will measure a particle charge and energy lower than the true one. In the case of a small angle of incidence, detected energy of the particle is equal to the true energy but its charge is higher than the true one. This is due to the fact that the particle track has a certain angle of inclination with respect to the electric field and its projection on the anode results in a height of the Bragg peak higher than is the case when the particle entered the detector parallel to the electric field lines. Oblique tracks can be minimized by the use of a properly designed collimator which allows the particle beam to enter the active volume of the detector parallel to the electric field or with a small incidence angle.

The particle range should be more than the grid–anode distance and less than or equal to the cathode–grid distance.

The particle should have energy in excess of 1 MeV/amu.

3. EXPERIMENTAL

3.1. BCS Detector

The basic components of the BCS detector namely, copper cathode, field shaping rings, grid, and gold-plated anode are mounted in an aluminum cylinder. The cathode–grid distance is 28.5 cm while the grid–

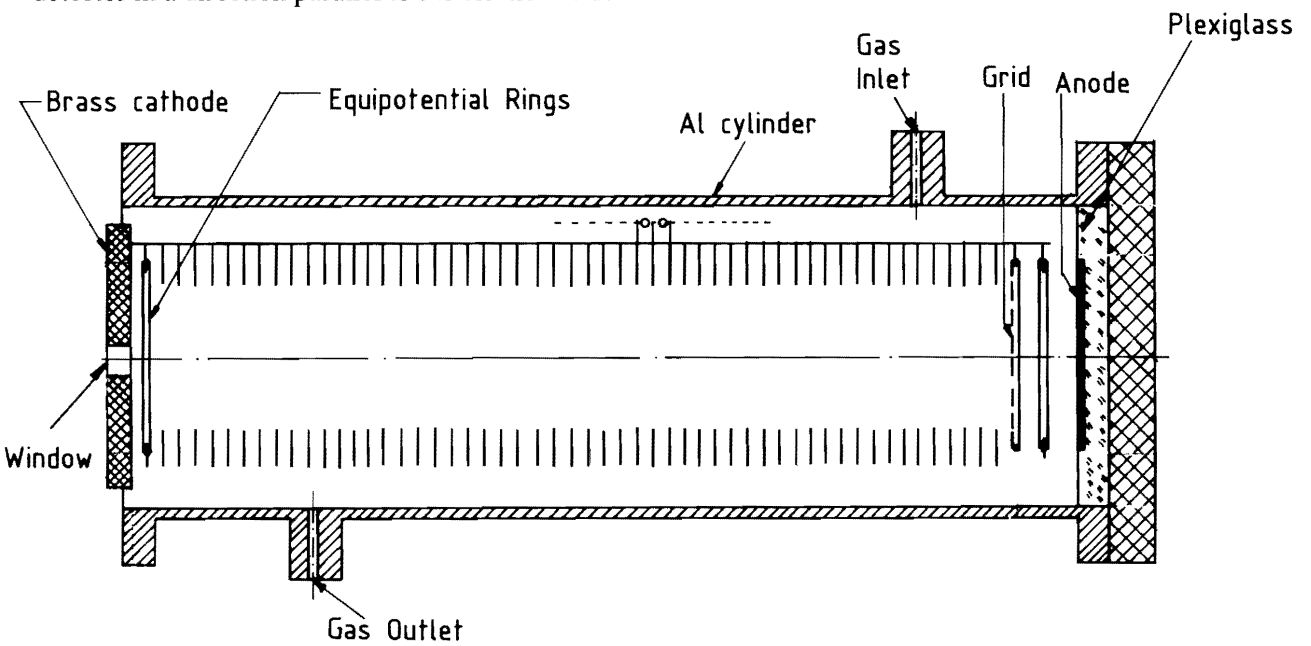

Figure 4. The design of the BCS detector

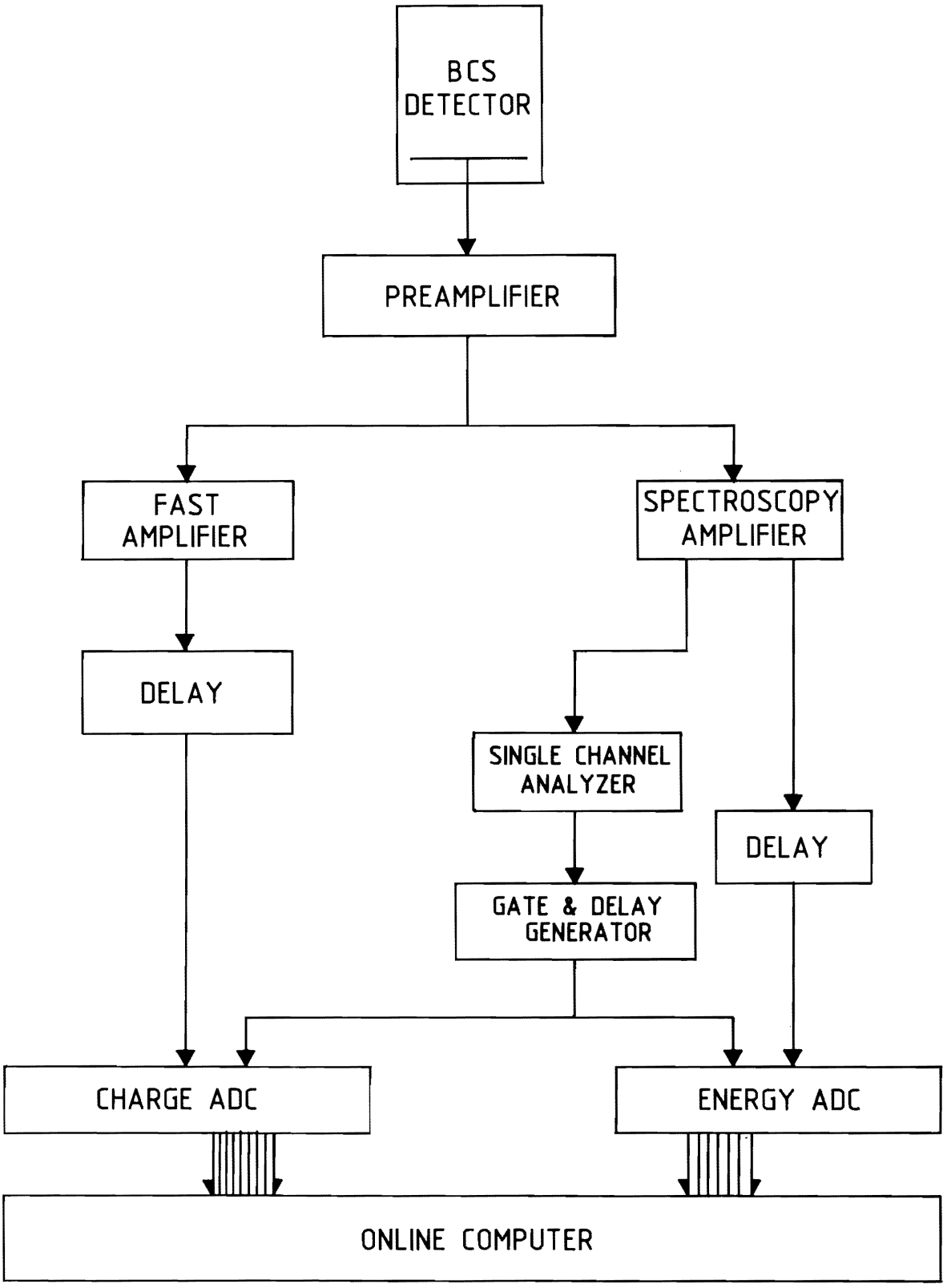

Figure 5. Block diagram of electronics used in the experiment.

Table 2. Optimum Operational Parameters of BCS Detector.

Gas Flow rate	10 l h^{-1}
Gas Pressure	200 torr
Cathode-Anode Potential Difference	1750 V
Reduced Electric Fields:	
Cathode to grid	0.25 V cm^{-1} $torr^{-1}$
Grid to anode	0.65 V cm^{-1} $torr^{-1}$
Shaping Times:	
E-Signal	1 ms
Z-Signal	0.25 ms

anode distance is 2.1 cm. A hole 1 cm in diameter in the cathode allows the particle to enter the active volume of the detector. A polypropylene foil, having a thickness of 145 μg cm^{-2}, is stretched on the cathode hole so that the detector, which operates at higher gas pressure, can be used in vacuum inside a scattering chamber and the particle can enter the detector without significant energy loss. Uniform potential gradient was maintained between the cathode and anode using equipotential rings, as shown in Figure 4. The grid is a mesh of wires with 20 μm thickness and separated by 1 mm. The inefficiency of the grid was calculated using the formula given in reference [4] and was found to be 0.0157. This detector was built at the Physics Department, Krakov University, Poland and was modified at the Cyclotron Laboratory, Institute of Experimental Nuclear Physics, IKIII, Kernforschungzentrum, Karlsruhe, Germany. These performance tests were also carried out in the same laboratory. The optimum operational parameters of BCS detector, determined in a series of bench tests are summarized in Table 2.

3.2. Electronics and Data Acquisition System

The anode signal was fed to a charge sensitive preamplifier. Later on this signal was splitted into two branches for energy and charge analysis. The energy signal was processed by an amplifier with a shaping time of 1 μs while charge signal was processed by an amplifier with shaping time of 0.25 μs. Energy and charge information were digitized into 8192 channels and were stored event by event on a magnetic tape using an online NOVA2 computer. Figure 5 shows the block diagram of electronics used for the detector tests.

4. BCS DETECTOR PERFORMANCE TESTS

4.1. Detector Tests of Oblique Tracks

As mentioned in section 2.3 oblique tracks result in tailing in the charge and energy spectra of completely stopped particle in the detector. This effect was thoroughly studied with uncollimated and collimated beams of alpha particles from a mixed nuclei source. The alpha source contained ^{239}Pu, ^{241}Am, and ^{244}Cf nuclei which emit alpha particles with 5.2, 5.5, and 5.8 MeV energies respectively. In order to get uncollimated beam of alpha particles, source was mounted inside the detector on the inner side of cathode facing the anode. The correlated energy and charge spectrum of uncollimated alpha particles is shown in Figure 6. The three alpha peaks are quite prominent at the end of the continum caused by oblique tracks. The ratio of peak of the continum to the three alpha energy peaks is very large and is measured to be 4.8. Ideally this ratio should be zero. In the second part of the study the alpha source was mounted in specially designed long collimator, which allowed alpha beam to enter the detector parallel to the electric field axis. Figure 7 shows correlated energy-charge spectrum for collimated beam of alpha particles, which is almost background free. The small background in the continum region is due to particles which are not completely stopped in the active volume of the detector. Figures 8 and 9 show the charge and energy spectra of the detector for collimated beam of 5.2, 5.5, and 5.8 MeV alpha particles. The measured energy resolution of the detector for three alpha energies is 1.5% while corresponding charge resolution is 3%.

4.2. Detector Tests with ^{4}He + ^{27}Al reaction

The response of the BCS detector for light ions was tested using ^{4}He + ^{27}Al reaction products emitted at 30 degree lab. angle. This reaction was chosen because its products have energy in excess of 1 MeV/amu. These tests were performed at the Cyclotron Laboratory, Institute of Nuclear Physics IKIII, Kernforschungzentrum, Karlsruhe, Germany. In these experiments, 1.5 and 6.3 μm thick aluminum foils were used as targets. The detector was placed 30 cm away from the target and its anode subtended a solid angle of 0.14 millisteradian at the target. The experiment was carried out using a 90 nA current of alpha particle beam at 104 MeV energy.

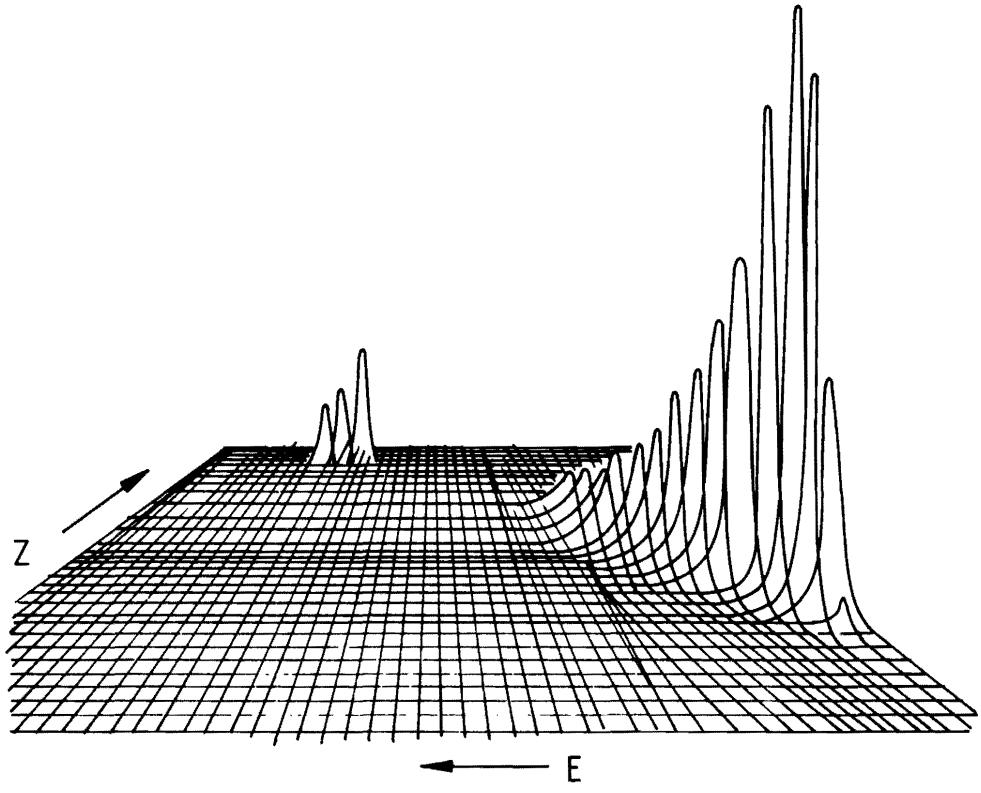

Figure 6. Three-dimensional spectrum of the energy and charge of the alpha particles obtained by the BCS detector without a collimator. Three peaks are well resolved. The high ridge is the effect of the oblique tracks.

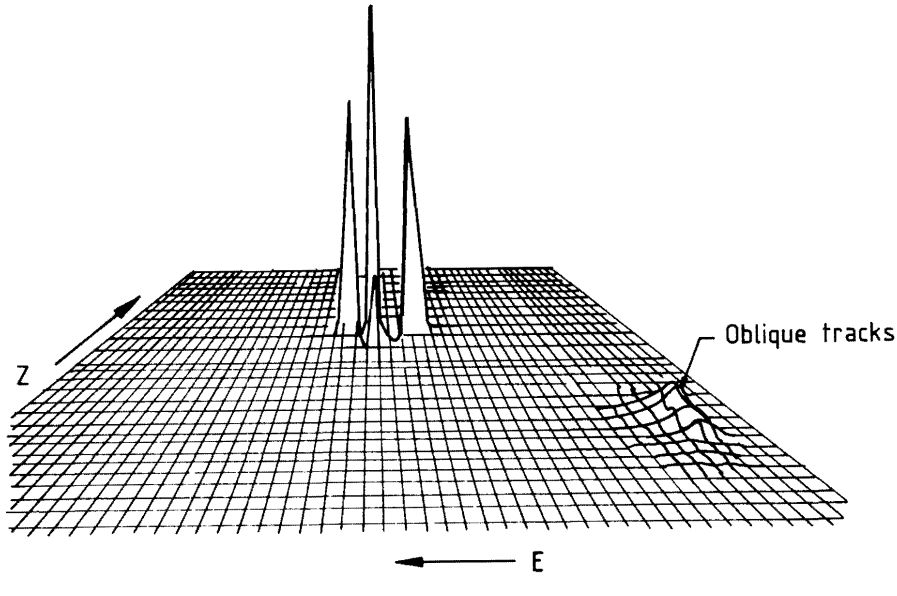

Figure 7. Three-dimensional spectrum of the energy and charge of the alpha particles obtained by the BCS detector with the collimator. The three peaks are well resolved. The high ridge which is observed without the collimator has clearly disappeared.

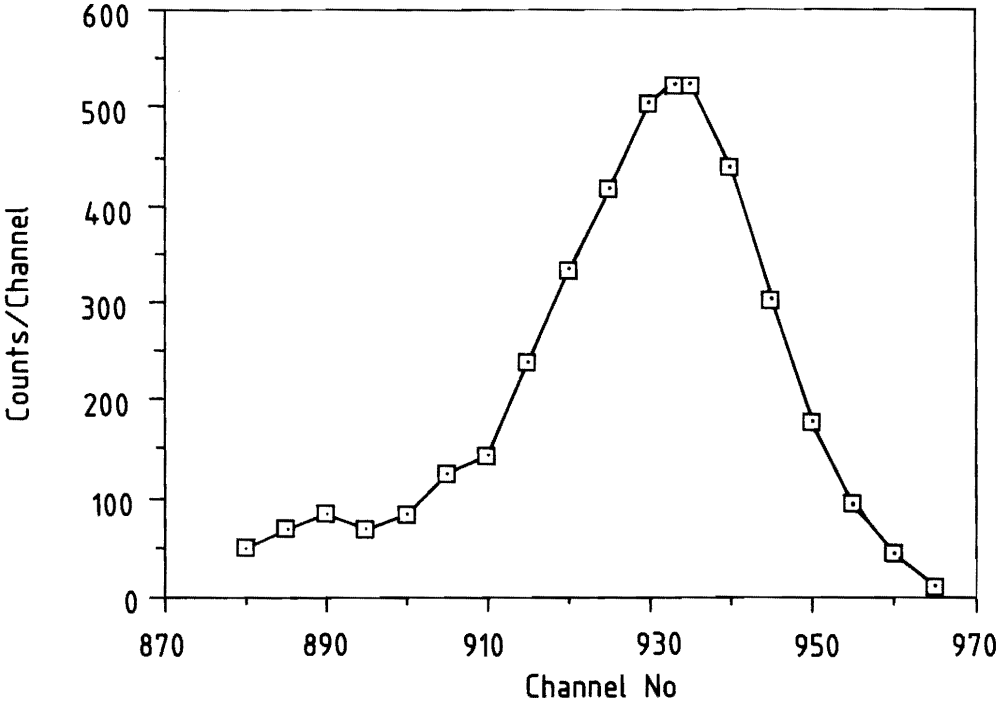

Figure 8. Charge spectrum of alpha particles taken by BCS Detector.

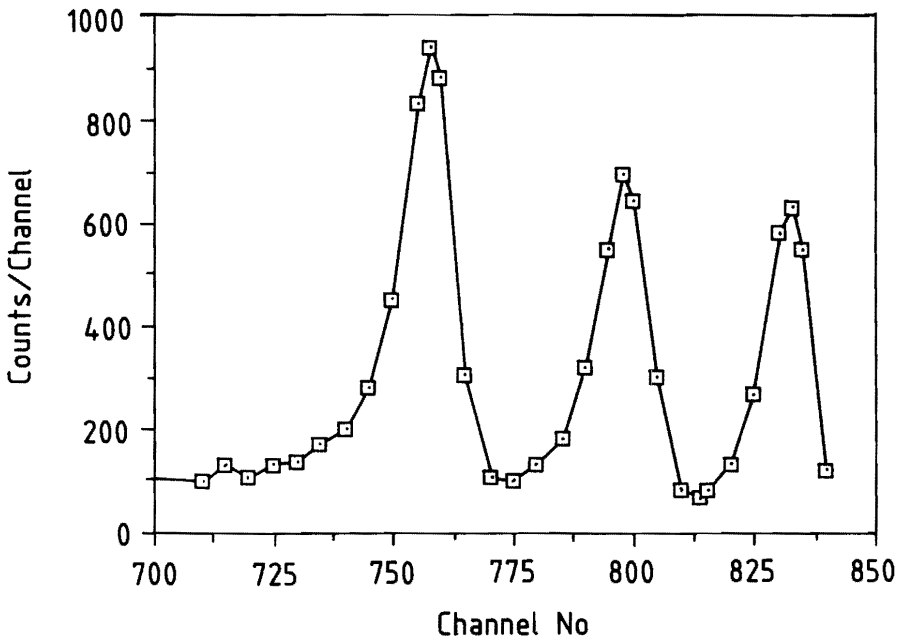

Figure 9. Energy calibration spectrum of BCS detector using alpha source.

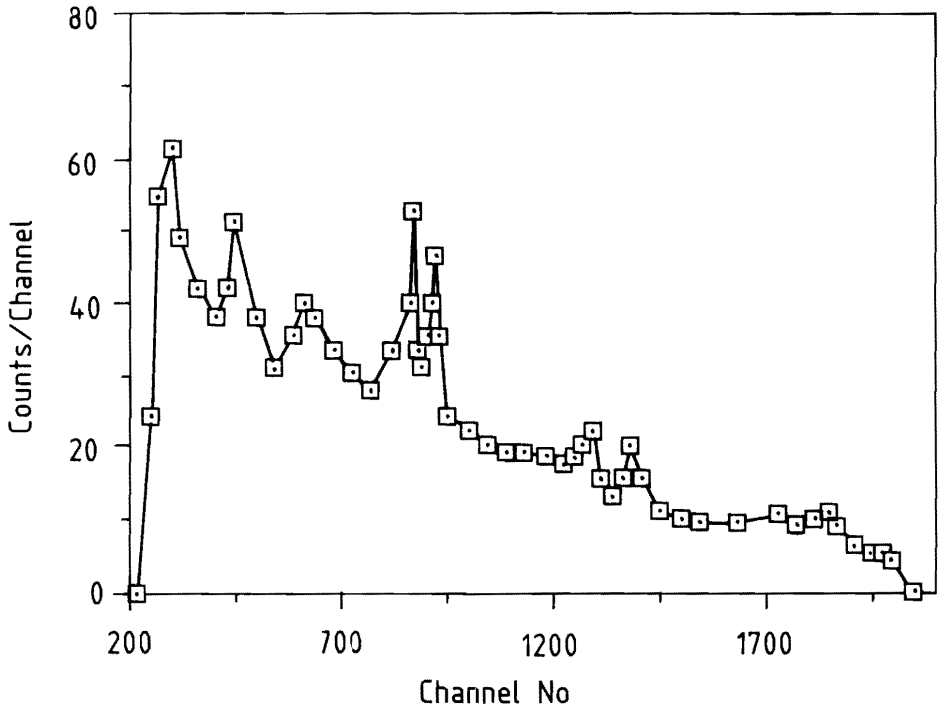

Figure 10. The energy spectrum of the products of Al(α, X) reaction.

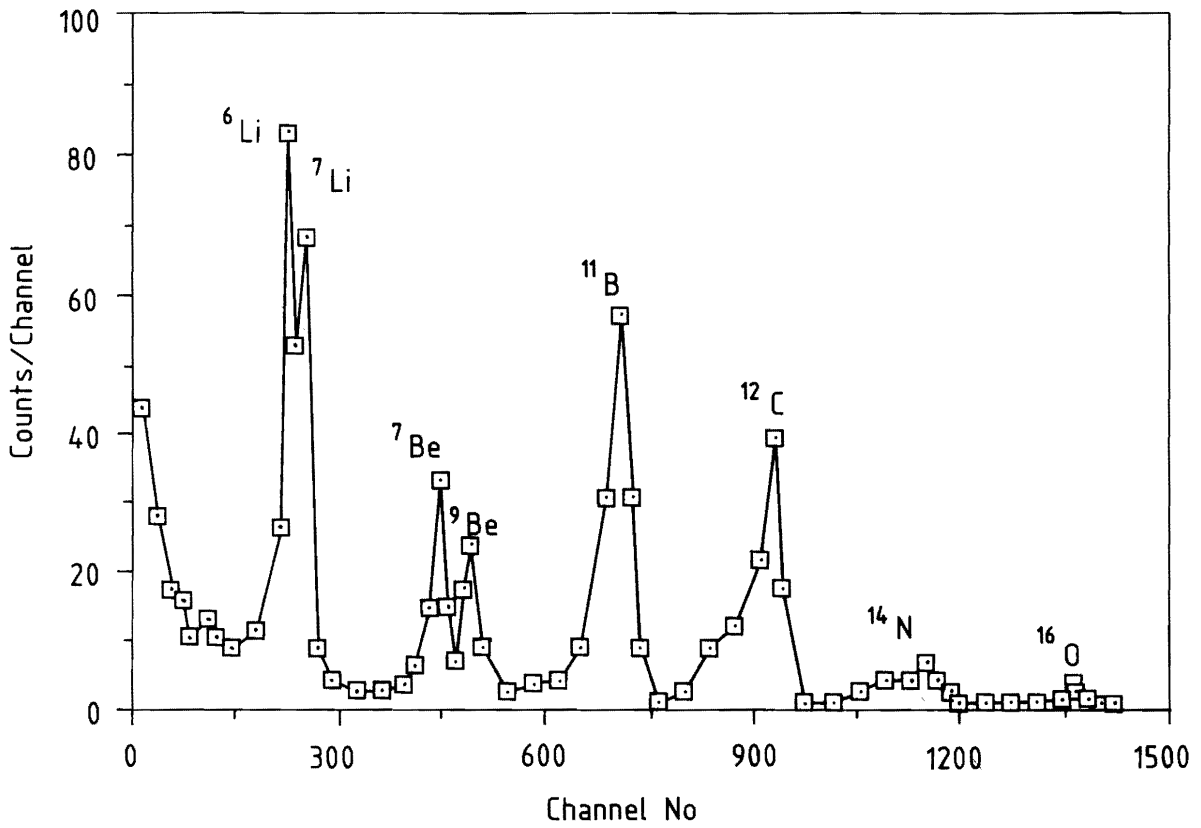

Figure 11. Charge spectrum of the products of Al(α, X) reaction.

4.2.1. Results of Tests with $^{4}He + ^{27}Al$ reaction

The IBM computer of KFUPM was used to analyze the data written on the magnetic tape. The energy and charge events were sorted out in 2048 channels each. Figures 10 and 11 show the energy and charge spectra of the reaction products, respectively. The energy spectrum shows a continuous energy distribution along with the peaks due to background from scattered incident beam. Figure 11 shows the charge spectrum with prominent peaks. In order to find the correlation between energy and charge for various ions, E and Z events were sorted out in a 100 $\times$ 100 matrix, as shown in Figure 12. In order to provide better view, the matrix is rotated such that the origin is on the farther right corner of the figure. The noticeable features of Figure 12 are its almost equidistant peaks along Z-axis corresponding to discrete charges. All of these peaks originate from a point lying under the continum ridge. The high ridge at the farther right corner is due to low energy and charge background events. These low energy and charge events are produced by those particles which have either energy less than 1MeV/amu or have oblique tracks or are not stopped in the detector. The curving of these ridges at their beginning is due to ions having energies less than 1 MeV/amu. It is noticed that each ridge ends on peak, which is caused by summation of channels. The small tail at the end of each ridge, which is extended toward lower energies and lower charges, is due to those particles which are not completely stopped in the detector.

The charge of the particle detected in the BCS detector can be identified by knowing the energy deposited by the particle in the detector. The minimum energy deposited by a particle, in order to be detected by the BCS detector is 1 MeV/amu while for maximum energy, the range of particle should be equal to 28.0 cm, the effective length of the detector. Using the data from reference [8], we have calculated the minimum and maximum energies of ^{7}Li, ^{9}Be, ^{11}B, ^{12}C, ^{14}N, and ^{16}O ions which can be stopped in our detector. These values are shown in Table 3. In order

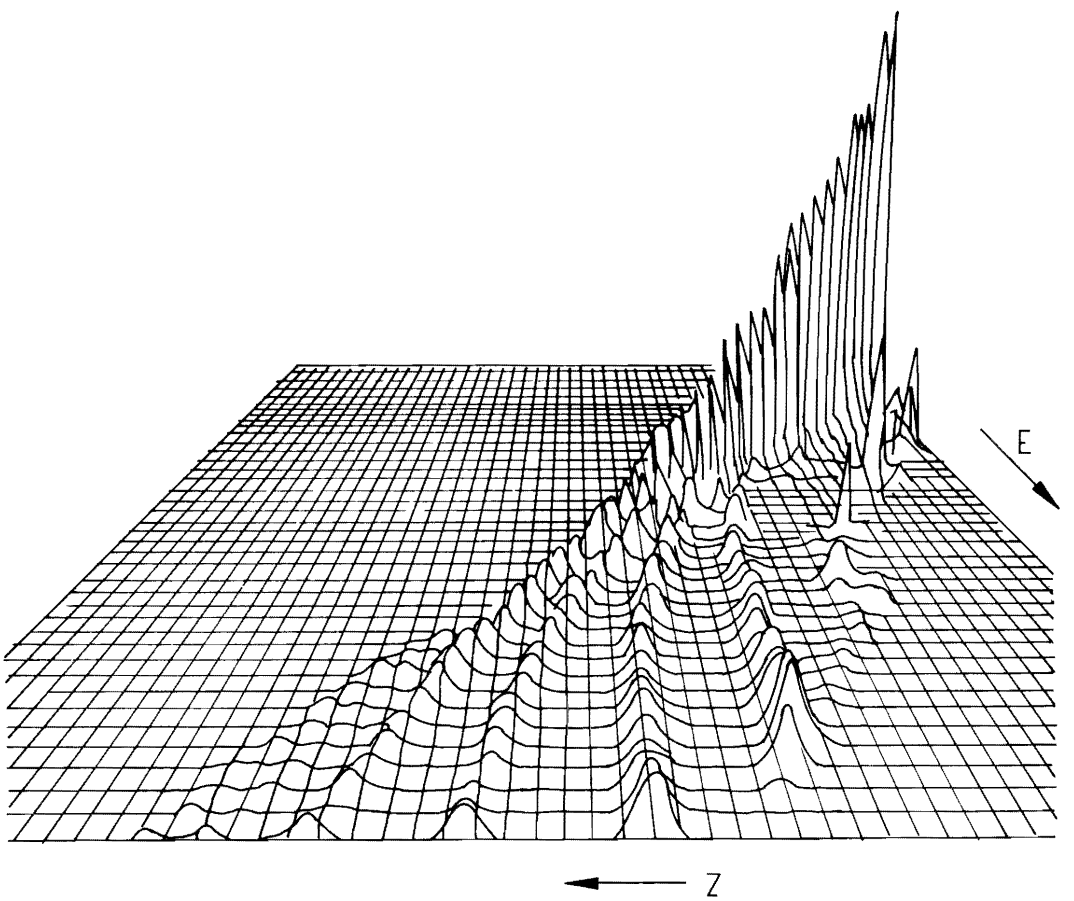

Figure 12. A three-dimensional spectrum of E and Z of the products of $^{4}He + ^{27}Al$ reaction.

to identify the charge for discrete Z peaks, the energy distribution of reaction products corresponding to each Z peak was plotted and the minimum and maximum energy of the spectrum was calculated using the energy calibration lines from the alpha source. Figure 13 shows the energy spectrum corresponding to the first peak, which has a minimum energy of 6–7 MeV and a maximum energy of 14–15 MeV. Comparison with Table 3 reveals that this peak is ^{7}Li peak. Similarly, ^{9}Be, ^{11}B, ^{12}C, ^{14}N, and ^{16}O peaks were identified.

Table 3. Charge Resolution of BCS Detector.

Ref.	Ions	Z	Ions Energy (MeV)		$\Delta Z/Z$ (%)
			Min.	Max.	
Present Work	^{4}He	2	4	5.0	3.1 + 0.1
	^{7}Li	3	7	14.7	2.6 + 0.3
	^{9}Be	4	9	22.2	2.7 + 0.5
	^{11}B	5	11	30.5	3.4 + 0.2
	^{12}C	6	12	34.0	3.6 + 0.3
	^{14}N	7	14	39.2	3.8 + 0.5
	^{16}O	8	16	49.4	4.1 + 0.4
Fruhn et al. [5]		10	–	–	1.6
		26	–	–	1.4
Schiessel et al. [6]		16	–	–	1.4
Asselineau et al. [7]		18	–	–	2.7

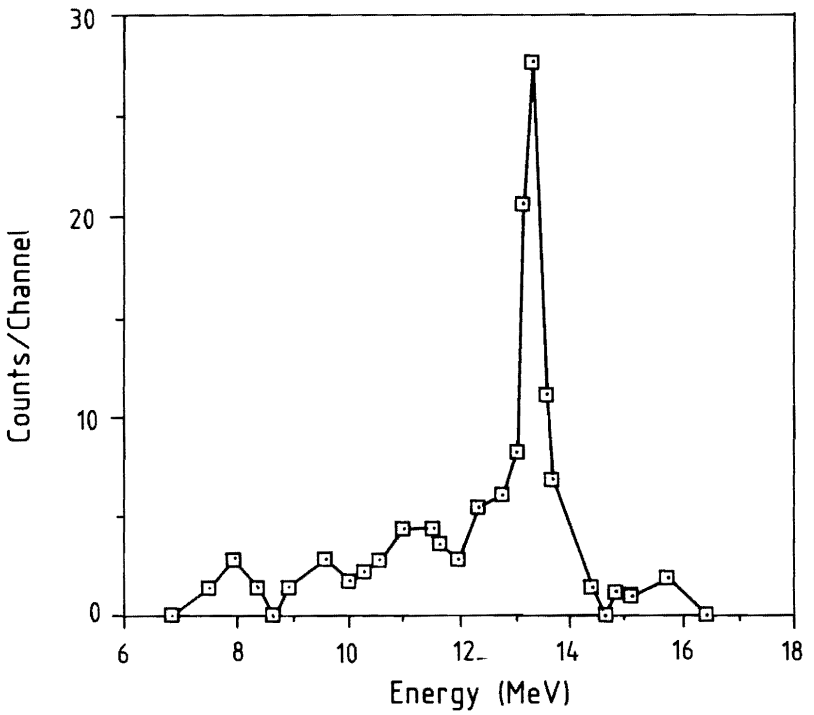

Figure 13. The energy spectrum gated with first peak in Z spectrum.

As shown in Figure 11 Li and Be peaks show doublets. One can exclude the effects of electronics as a cause of this doubling. These doublets might be assigned to different isotopes of Li and Be produced in $^{4}He + ^{27}Al$ reaction. Hornyak *et al.* [11] have measured the yield of ^{6}Li, ^{7}Li, ^{7}Be, and ^{9}Be isotopes in $^{4}He + ^{27}Al$ reaction at 140 MeV energy. If one considers the mass dependence of specific energy loss dE/dX, one expects slightly different height of Bragg peak for different isotopes. The difference should be proportional to the mass difference. The separation between the Be doublet is twice that of Li doublet. This means if the mass difference between Li ions is one then Be ions have a mass difference of two. Therefore one can identify ^{6}Li and ^{7}Li in the Li peak while ^{7}Be and ^{9}Be can be assigned to the Be doublet.

The charge resolution of the BCS detector for light ions ^{7}Li, ^{9}Be, ^{11}B, ^{12}C, ^{14}N, and ^{16}O, measured in this experiment, is tabulated in Table 3. It varies from $2.6 + 0.3\%$ for ^{7}Li to $4.1 + 0.3\%$ for ^{16}O. For the sake of comparison, we have also included the similar data from references [5–7] in Table 3. Gruhn *et al.* [5] and Shiessel *et al.* [6] have reported charge resolution better than our results because they have operated the detector at higher gas pressure. Our data is consistent with the results of Asselineau *et al.* [7]. These tests have revealed that the BCS detector has good charge resolution for light ions.

5. SUMMARY

Performance tests of a BCS detector have been carried out using $^{4}He + ^{27}Al$ reaction at 104 MeV energy. The effect of oblique tracks on the detector performance was investigated in bench tests using alpha source. The charge and energy resolution of BCS detector have been measured for light ions ranging from Li to O. The measured energy resolution of the detector for light ions is 1.5% while charge resolution varies from 3–4%.

The authors wish to thank the staff of the Cyclotron Laboratory and Prof. Dr. H. Rebel for their valuable help during this experiment. Financial assistance from KFUPM is gratefully acknowledged.

REFERENCES

[1] G. Sieger, H. Wollrick, J. Greif, G. Fiedler, M. Asghar, G. Bailleut, J. P. Bocquet, J. P. Gautheron, H. Schrader, H. Ewald, and P. Armbuster, *Phys. Lett.*, **53B** (1974), p. 45.

[2] H. G. Clerc, K. H. Schmidt, H. Wohlfarth, W. Lang, H. Schrader, K. E. Pferdekamper, R. Jungmann, M. Asghar, J. P. Bocquet, and G. Siegert, *Nucl. Instr. and Meth.*, **124** (1975), p. 607.

[3] U. Quade, K. Rudolph, and G. Siegert, *Nucl. Instr. and Meth.*, **164** (1979), p. 435.

[4] H. W. Fullbright, *Nucl. Instr. and Meth.* **162** (1979), p. 21.

[5] G. R. Gruhn, M. Binimi, R. Legrain, R. Lovemann, W. Pang, M. Roach, D. K. Scott, A. Shotter, T. J. Symons, J. Wonters, and Zisman, *Nucl. Instr. and Meth.*, **196** (1982), p. 33.

[6] Ch. Schiessel, W. Wagner, K. Hartel, P. Kientle, H. J. Korner, Waltrand Mayer, and K. E. Rehm, *Nucl. Instr. and Meth.*, **192** (1982), p. 291.

[7] J. M. Asselineau, J. Duchon, M. l'Haridon, P. Mosrin, R. Regimbart, and B. Tamin, *Nucl. Instr. and Meth.*, **204** (1982), p. 109.

[8] L. C. Northcliffe and R. F. Schilling, *Nucl. Data Tables*, **A7** (1970), p. 233.

[9] A. H. AI-Ramadhan, *Master Thesis, Physics Department, King Fahd University of Petroleum and Minerals, Dhahran, Saudi Arabia* (unpublished).

[10] D. M. Barrus and R. L. Blake, *Rev. Sci. Instrum.*, **48** (1977), p. 116.

[11] W. F. Hornyak, M. D. Glascock, C. C. Chang, and J. R. Wu, *Phy. Rev. C.*, **19** (1979), p. 1595.

Paper Received 28 October 1989; Revised 30 July 1990.